Scientific Report

Period 01/01/2013 – 31/12/2013

INAF – OAR for the Astrodeep project - First Periodic report



ASTRODEEP

"Unveiling the power of the deepest images of the Universe"

THEME [SPA.2012.2.1-01]

[Exploitation of space science and exploration data]

Grant agreement for: Collaborative project

Grant agreement no: 312725

ABSTRACT

In this document we present an overview of the project objectives in this first reporting period.

Prepared by: A. Fontana, K. Boutsia A. Comastri, S. Derriere, J. Dunlop, D. Elbaz.H. Ferguson
Approved by: AEC
Date: 27/02/2014

1 Project Objectives for this period 3
2 List of deliverables 4
3 WP3: Development and testing of algorithms. 4
3.1 Description and goals of WP3 4
3.2 Report on activities of WP3.2 5
3.2.1. Toward a new generation of TFIT *5*
3.2.2 The analysis of Herschel Images *6*
3.2.3 The analysis of the 4Ms Chandra image of the CDF-S *8*
WP4: Data processing and catalogue production 9
4.1 Description and goals of WP4 9
4.2 A revised ASTRODEEP data plan 9
4.3 Catalogues and Data 10
5. WP5: Science: The physics of early galaxy evolution 10
5.1 Description and goals of WP5 10
5.2 Results from first year. 11
6. WP6: Simulations of the Euclid deep survey 13
7. WP7: Dissemination and Outreach 13
7.1 Description and goals of WP7 13
7.2 The development of the ASTRODEEP web portal 14
7.3 The consortium meeting 14
8. Project management during this period 15
8.1 WP1: Management 15
8.2 WP2: Scientific Management 17
9. Appendices 20
9.1 Addendum to 3.2.1: Toward a new generation of TFIT 20
9.2 Addendum to 3.2.2: The analysis of Herschel images 26
Tuning and testing algorithms for object detection: getsources *26*
Tuning and testing algorithms for PSF-matching: *28*
FASTPHOT *28*
9.3 Addendum to 3.2.3 The analysis of the 4Ms Chandra image of the CDF-S 34

1 Project Objectives for this period

This report describes the achievements of the first year of ASTRODEEP.

ASTRODEEP is a coordinated and comprehensive program of *i)* algorithm/software development and testing; *ii)* data reduction/release, and *iii)* scientific data validation/analysis aimed at making Europe the world leader in the exploitation of the deepest multi-frequency astronomical survey data.

Our focus is on extra-galactic survey deep fields, i.e. those public observing programs motivated by the desire to understand the formation and evolution of galaxies and super-massive black holes from the very earliest times, and to answer fundamental questions in cosmology such as how and when the universe was re-ionized. They include data from space, notably from HST, XMM, Herschel and Spitzer, and from several optical and far-IR ground-based facilities. The main technical problems we seek to overcome relate to the varying depth and, most importantly, widely varying angular resolution of the data delivered by observatories working over a wide range of frequencies.

The focus of this project is on bringing together the expertise of our team to **i)** develop, refine and combine advanced algorithms for data analysis, **ii)** test and properly validate their effectiveness on the deepest multi-frequency data in tandem with scientific analysis, and **iii)** apply these validated tools to produce uniquely powerful homogenized data products for further scientific exploitation by the worldwide astronomical research community.

As described in the original proposal, ASTRODEEP is designed to achieve its major results within a timescale of three years. However, as appreciated and agreed during the negotiation phase, the goals of ASTRODEEP cannot reasonably be achieved in the first three *calendar* years of the project, simply because the recruitment of the best available young researchers inevitably takes several months, and some further time is required for these new staff to get up to speed and become effective within the project. For this reason, ASTRODEEP is planned to extend over a period of four years, although the funds are designed to sustain its full operations for three years as originally planned.

Despite this rescheduling of our plan, we decided to maintain the first reporting period and its review at the end of the first year, in an effort to ensure that ASTRODEEP gains momentum as quickly as possible, and to provide a means of verifying that early progress is being made.

As we discuss in more detail below, our main objectives for this first period were to:

- Advertise for and recruit new young researchers (at all three sites) with the necessary scientific ability and technical skills to drive the project forward and ultimately achieve our objectives; these are key appointments, as these young researchers in effect constitute the major investment of ASTRODEEP;
- Undertake a comparative assessment of the different approaches and techniques utilised for multi-frequency data analysis within our own research groups, and indeed within other leading research groups worldwide;
- Further explore the efficiency and effectiveness of these existing data-analysis methods, and commence the process of developing more advanced methods which can potentially combine the best features of existing algorithms and codes;
- Update and upgrade our plan for data processing, including the latest surveys that have been approved and/or commenced since submission of the original proposal;

- Establish the collaboration tools and research/dissemination environment required for the ASTRODEEP project.

We have successfully completed the recruitment exercise, with all key personnel in place by summer 2013. This we regard as our major achievement, as we are convinced that, despite (or perhaps because of) the duel technical/scientific demands of ASTRODEEP, we are convinced that we have been able to attract and secure very talented young researchers whom we are confident will be able to make a significant contribution to ASTRODEEP.

All the others activities have also started and are well tracked. We have already achieved significant results in improving the current software and in developing new approaches to data analysis. This rapid start to the project provides us with additional confidence that ASTRODEEP will be able to achieve its planned results.

The recent approval of new deep surveys, such as the HST Frontier Fields Initiative, the ALMA Deep Field, and the Spitzer SPLASH project, as well as continued support for on-going major surveys such as HST CANDELS and UltraVISTA, guarantees a continued flow of new and exciting multi-frequency data to which we will apply our analysis tools. We have therefore prepared a new plan to analyse these data. We anticipate that the homogenised catalogues we will produce from these ground-breaking surveys will guarantee that the ASTRODEEP project has a high and long-lasting scientific impact.

We summarize below the major achievements of each scientific Work Package. For each of them, we refer to the Appendices or to separate relevant associated documents for full details.

2 List of deliverables

Deliverable number	**Deliverable Title**	**Delivery Date**	**Status**
D1.1	Methodology for the emission of the calls for scientific consultants	T0+4 months	Delivered
D2.1	Management Portal (internal to consortium)	T0+6 months	Delivered
D3.1	Scientific report on existing software	T0+12 months	Delivered
D4.1	Survey on available data and planning of catalogue release	T0+6 months	Delivered
D5.1	List of science papers #1	T0+12 months	Delivered
D7.1	Beta release of public web portal	T0+6 months	Delivered
D7.2	Public release of public web portal	T0+12 months	Delayed – expected T0+15 months
D7.3	Call for collaboration meeting	T0+11 months	Delivered

3 WP3: Development and testing of algorithms.

3.1 Description and goals of WP3

The main objective of this WP is to develop and test algorithms for image detection, de-confusion and photometry in deep and crowded extragalactic fields.

The main objectives of this WP as described in the DoW are:

- Tune and test algorithms for object detection
- Tune and test PSF-matching methods
- Explore and test other techniques for multi-band photometry: matched aperture photometry, cross correlation, etc
- Compare different recipes in an effort to understand and quantify the differences.
- Properly code the public software that will eventually be released, based on the combined evolution of CONVPHOT and TFIT.
- Develop proper tools for the handling of Grism spectroscopic data collected with WFC3.

Deliverables expected in the period are:

- D3.1 Scientific report on existing software

3.2 Report on activities of WP3.2

This has been one of the most active WPs. In this first year we accomplished the results summarised below.

3.2.1. Toward a new generation of TFIT

The goal The first goal has been to compare the various PSF-fitting codes that we currently use within our research teams (TFIT, CONVPHOT, McLure's, MEGAD) that use prior information from high-resolution (usually HST) images to perform matched photometric measurements in ground-based and Spitzer-IRAC images. This comparison has been performed at a deep (source code) level, in order to identify the differences and similarities. After a comparison at the level of code details, we have decided to create a new software package that combines the best ingredients of all these individual techniques and codes. To make progress we have decided to focus first on the codes that use the actual galaxy profiles observed at high resolution as priors, deferring possible further exploration of the technique of fitting functions to each galaxy (as currently implemented in MEGAD; Buitrago et al. in prep, and PyGFIT; Mancone et al. 2013 PASP125, 1514) to a later version of our code.

TPHOT A first brand-new version of our proposed new software has already been completely written. This new code is currently dubbed TPHOT, to emphasize that it is primarily based on TFIT and CONVPHOT, but it will be eventually released under another name. In practice, we have re-written the kernel code of TFIT in C, substituting (and fixing bugs within) the previous Python routines that were used to perform the numerically intensive computations in TFIT. We have also implemented within the code several alternative methods of performing the same operation, and these options can be selected by the user when running the code. This allows us to test the effectiveness of various options within the same code.

TPHOT has been thoroughly tested and shown to obtain exactly the same results as TFIT or CONVPHOT, when used in the same manner as the original code.
The optimization of the code has produced an impressive increase in computing speed, by an order of 30x in the case of TFIT, and of 2x in the case of CONVPHOT. The former figure of merit is essentially due to the enhanced speed of the C code as compared to the original Python implementation. The latter improvement over the original efficiency of CONVPHOT is

primarily due to use of a faster convolution technique, although several other improvements have also been achieved.

Simulation tool We have developed a tool to create simulated images, with realistic galaxy sizes, number densities and colours, along with angular resolution and noise levels/characteristics as appropriate for the datasets we ultimately plan to analyse. This simulation tool enables us to prepare simulated images both in simple geometrical configurations (e.g. blends of two galaxies of variable flux, morphology and distance) as well as a fully realistic deep field.

Testing TPHOT Using this image simulator we have already started to test TPHOT with implementation of its various options. We have already identified a number of critical issues, i.e. cases where current implementation fails. As an example, current results suggest that in a typical run of TFIT about 1-2% of the sources have a severe error on the estimated photometry. We have already verified that the critical issue is the specific minimization procedure adopted: exact minimization (as used in CONVPHOT) leads to correct results but is computationally intensive and slows significantly the code; the "smart" solution implemented in TFIT is prone to severe errors in some unfortunate configurations. We need to finish our extensive tests on simulated images not only to identify severe errors but also small biases and systematic errors that may be produced in the various configurations.

Final remarks and future plan *We emphasize that, per se, the complete re-writing of TFIT into TPHOT, producing a code that is 30x faster, is already a major technical achievement.* The main limitation of TFIT is indeed its relative slowness: for instance, a typical run on a single CANDELS image takes about 1 day to be completed. This makes it impossible (at least for a normal research group) to perform the extensive simulations that are necessary to characterize the systematic effects in the various wavebands, simulations that require hundreds (or even thousands) of random realizations to properly sample the required parameter space. TPHOT makes this necessary step feasible. We are, however, part of the way through the development and further testing of the new TPHOT code, and indeed we now have ambitious plans for further improvements throughout the rest of the project before we deliver the final version of the code. The planned activities are:

- To obtain a full characterization of the expected biases and systematic errors in a wide range of expected configurations;
- To remove the sources of severe errors in the output photometry;
- To identify the most reliable implementation of the code;
- To integrate the possibility of using analytic fits to the observed galaxies instead of the directly observed luminosity profiles, in order to allow for the possibility of wavelength dependent morphologies, such as the real colour gradients displayed by galaxies;
- Release to the community the final version, that is expected to be significantly faster, substantially more robust, and undoubtedly more user-friendly than the current version.

Further details are given in Section 9.1.

3.2.2 The analysis of Herschel Images

The analysis of Herschel and other sub-mm images is very difficult because of the very poor spatial resolution, and because of the inherent errors of the positional information on the

detected sources. We are exploring a range of possible solutions.

Direct source detection with *Getsources*, a detection code that does not use prior information, but directly applies a multi-resolution blind source detection algorithm. *Getsources* has been developed primarily for large far-infrared surveys of Galactic star-forming regions with Herschel, but can also be applied to deep extragalactic surveys.
The model is described in the peer-reviewed refereed paper Men'shchikov et al. (2012, A&A 542, 81). Instead of following the traditional approach of extracting sources directly in the observed images, *Getsources* analyzes filtered single-scale decompositions of detection images over a wide range of spatial scales (separated by only 5% in spatial scales) and across all wavelengths.
We have extensively tested *Getsources* on simulated images that closely reproduce the image quality and depth of the Herchel CANDELS images. We have been able to show that in the PACS 100μm and 160μm bands, at least 68% of the sources can be extracted with photometry accurate to better than 32% above 1 mJy and 4mJy respectively. This is comparable to the confusion limits derived by Elbaz et al. (2011, A&A 533, 119) in these bands. However, the error on recovered fluxes becomes more and more significant in the SPIRE bands with increasing wavelength, suggesting that over-estimation of flux densities due to confusion with bright nearby sources remains a major issue especially at 350 and 500μm.
Using the same simulations we also compared the catalogues obtained with *Getsources* with those derived using 24 μm priors, as reported in Elbaz et al. (2011). We find that the limit of acceptable photometric reliability is typically two times larger (i.e. at flux densities 2x shallower) than the ones obtained in the catalogues extracted using 24 μm priors, since at faint flux densities spurious sources and confusion start to play a significant role. This demonstrates that the catalogues extracted with 24 μm positional priors are deeper than those produced by *Getsources* and retrieve faint sources with a significantly greater reliability.

Prior fitting with FASTPHOT. FASTPHOT is a quick and simple PSF fitting routine optimized for prior extraction (i.e. where the potential positions of the sources are known). It is conceptually similar to TFIT, the main difference being that it assumes that all objects are PSF-like, an acceptable approximation at Herschel (and JCMT) resolution. FASTPHOT was first developed by Béthermin et al. (2010, A&A, 516, 43), has been widely applied on Herschel data, and is publicly available at (http://www.ias.u-psud.fr/irgalaxies).
We have extensively tested FASTPHOT using the same simulated images described above, that reproduce the data depth and quality of the GOODS-N field.
We have been able to quantify the photometric accuracy of FASTPHOT as a function of source flux density, and have derived limits on the de-confusion capabilities within the various bands.
We have also developed a technique (that is adopted also by CONVPHOT) that improves the accuracy and reduces outliers by rejecting sources that have a (unphysical) best-fitting flux density that is negative. We explicitly show that this procedure improves the quality of the overall fit when compared with a similar technique by Chary, Magnelli et al. We also show that FASTPHOT is more effective in achieving a good completeness when compared to other tools based on the density of sources within a 20" radius in the 24μm catalogue.
Finally, we have verified that FASTPHOT accurately computes the photometric error as based on the covariance matrix.

Further details are given in Section 9.2.

3.2.3 The analysis of the 4Ms Chandra image of the CDF-S

The 4Ms image of the Chandra Deep Field South (that contains the GOODS-South field at its center) is currently the deepest X-ray image of the Universe, and hence provides our best laboratory for the study of faint AGNs and galaxies with extreme star-formation rates that can be detected in the X ray images. We have commenced our work in this area by first improving the techniques for background subtraction.

Building on our previous expertise on the analysis of X-ray data, we have not only re-analyzed the Chandra image with existing software, but also tested for the first time the concept of prior photometry on X-ray data. We compared our findings with the current reference catalogue in the 4Ms data, namely the one published by Xue et al. (2012, ApJ 759, 129), a classic blind wavelet detection method obtained with the CXC software *wavdetect*.

Background subtraction.

Previously the background map was computed with a spline fit to the source-subtracted image. This method left spurious features in the background maps and therefore we decided to make use of the background templates provided by the Chandra X-ray data Center (CXC). These are long exposures taken with the ACIS detector in stow mode so the only recorded events are instrumental events and particle background events. The remaining part of the background (purely cosmic diffuse background), that suffers from off-axis dependent vignetting, has been modeled according to the exposure map. A full description of the method can be found in Cappelluti et al. (2013, ApJ 769, 68).

Bind-source detection with *cmldetect* photometry.

As noted in several papers, wavelet detection methods (such as those used by *wavdetect*) are more accurate in determining positions, but are unable to detect the faintest sources. In addition, the photometry provided by *wavdetect* is less accurate than that achieved with the PSF-fitting method adopted by *cmldetect.* To improve on these two aspects, we have performed a more aggressive detection by pre-selecting a large number of background fluctuations isolated by a sliding cell technique with a signal-to-noise ratio threshold SNR=2. The pre-selected sources have then been fitted with *cmldetect* with the position, flux and extension as free parameters. A comparison with the X2 catalog shows that we nearly double the number of faint sources, significantly increasing the completeness at the faintest limits.

Prior detection using HST catalogs

As a further step, we have used the full optical-nearIR catalogue of Guo et al (2013, ApJS, 207, 24), where the detection is done on the ultradeep CANDELS H-band images, as a prior for the X-ray object detection and use *cmldetect* to perform the photometry on the Chandra images. This is analogous to the procedure adopted to obtain the Spitzer-IRAC photometry in the CANDELS field, but in this case using a software routine (*cmldetect*) that is already optimized for X-ray images. We have shown that by using this approach we have been able to detect additional faint X-ray sources that escaped detection in the previous catalogues. In a forthcoming report we will report on the optical identifications and the selection function of the new catalogue.

Further details are given in Section 9.3.

WP4: Data processing and catalogue production

4.1 Description and goals of WP4

The main objective of this WP is to deliver high quality multi-wavelength catalogues extracted from space and ground-based datasets, using the algorithms developed in WP3.
In this early stage, only preliminary results are expected, using the algorithms already available, while the new generation of algorithms and codes are being developed.

The main activity for this period has been an update of the plan for data processing.

Deliverables expected in the period are:

- Report on available data and planning of catalogue release (D4.1)

4.2 A revised ASTRODEEP data plan

We have revised the original list of data sets that we plan to analyze beyond the original list that was included in the submitted ASTRODEEP proposal. This update is motivated by the need to properly align our plans with recent changes and improvements in the current and forthcoming public surveys. In our revision we have re-affirmed that our main focus remains on the data obtained in the five premiere extragalactic fields (GOODS-N and GOODS-S, UDS, COSMOS and EGS). We have revised the list of data in these fields by including the latest set of public and proprietary images.
In this context, the most noteworthy improvement has been the addition of the first ALMA deep field, a new project (led by J. Dunlop) that is starting now and will deliver data in 2014.

The major additional update to our plan in terms of new fields results from our desire to include the new deep data that will be provided by the new Hubble Frontier Fields (FF) programme. This new, public programme commenced at the end of 2013 and will be completed in late 2015. It will ultimately deliver deep data over 12 different fields, 6 deliberately targeted on known high-redshift galaxy clusters, and 6 in nearby blank-field regions. Each field will be imaged in 8 HST bands to a depth comparable to the original Hubble Ultra Deep Field. The same fields will be also observed with Spitzer, providing mid-infrared imaging in the two available Spitzer Warm Mission IRAC bands. The rationale is to use the amplification provided by the gravitational lenses of the clusters to detect the (intrinsically) faintest galaxies in the epoch of re-ionization. It seems clear that these new deep fields will attract much of the interest from the high-redshift research community over the next years. At the moment no plan is currently funded from NASA or other public agencies to obtain high quality catalogues from these data. We further note that the analysis of these data is expected to present a particularly demanding challenge for source de-blending tools, given the large density of foreground sources which inevitably lie within the foreground lensing clusters, the complex shapes of gravitational lenses and the presence of a variable background due to intra-cluster light. We therefore believe that analysing the FF data and releasing the relevant de-confused catalogues is a challenging but important opportunity for the ASTRODEEP project to have a major and timely impact on the astronomical community.

In summary, the plan for coming years is:

- In 2014, to complete the release of the CANDELS, HERSCHEL and ALMA catalogues obtained with the current version of our codes;
- In late 2014 and in 2015, to use the revised versions of our codes to release the catalogues on the FF, as soon as they become available;

- In late 2015, to use the final version of our codes to deliver a final release of the CANDELS and HERSCHEL catalogues, if the additional value compared to the previous catalogues is deemed worthwhile in the context of the required effort.

4.3 Catalogues and Data

In this period we have assembled a limited number of new catalogues, since our prime objective has obviously been the improvement of the analysis software. However, we have (in parallel) been using our existing tools to assemble and/or improve existing catalogues within our key target survey fields. In particular we mention:

- In the GOODS-S field, the addition of the final K-band data provided by the VLT HUGS survey (e.g. Sommariva, 2014 A&A subm.) to the existing CANDELS catalogue (Guo et al. 2013). The new K-band imaging is significantly deeper than the original image used in Guo et al. (2013), and in addition now covers the full HST-WFC3 survey area. At present, the new K-band data have been processed with the current version of TFIT for homogeneity with the Guo et al. (2013) catalogue. This new improved catalogue will be published in Fontana et al. (2014, A&A subm.) (see below).
- In the same field, we have also included the new deep B-Band obtained with VIMOS (P.I. M. Nonino). Again these data are 1*mag* deeper than the current HST ACS B-band images and cover the whole CANDELS survey area. They have also been analyzed with TFIT. This catalog will be published in Fontana et al. (2014) (see below).
- Within the COSMOS field we have been working to utilize the K-band imaging provided by the first UltraVISTA data release (DR1; McCracken et al. 2012, A&A, 544,156) to produce a multi-wavelength catalogue including matched resolution (i.e. deconfused) IRAC band-1 and band-2 photometry extracted from the public S-COSMOS data using MEGAD. UltraVISTA DR2 has recently been completed, providing significantly deeper imaging over ~70% of the field. An early version of a new catalogue based on UltraVISTA DR2 has recently been exploited in the search for z ~ 7 galaxies presented in Bowler et al. (2014, MNRAS subm.). Now, however, substantially deeper Spitzer IRAC imaging is available in the COSMOS field as a result of the SPLASH programme (PI Capak), and we plan use both MEGAD and T-PHOT to produce a new matched-resolution multi-wavelength catalogue based on these data. We anticipate completion of this catalogue by the end of 2014.
- We have compiled a new catalog of X-ray sources in the 4Ms Chandra images of the CDF-S. This catalogue uses the prior information from HST imaging, as described above, and allows us to detect a larger fraction of the sources close to the detection limit. This will be published in a forthcoming paper (Cappelluti et al. 2014)
- We are actively assembling the multiwavelength catalogs on the Herschel-CANDELS survey. The planned release if for August 2014.

5. WP5: Science: The physics of early galaxy evolution

5.1 Description and goals of WP5

This WP is focused on the scientific analysis of the unique data set this project will produce. We will use a variety of statistical indicators to explore the properties of high-redshift galaxies and AGNs. The huge data set that we will compile will allow us to obtain high order statistical distributions of galaxies as a function of different quantities. We plan to derive luminosity and

mass functions at different redshifts, correlation functions and other indicators of large-scale structures. We will explore the rest frame physical properties of galaxies (rest frame luminosities, masses, star-formation rates, morphologies) as a function of cosmic time, environment and spectral type. We will obtain a full census of AGNs at high redshift, including those most absorbed, and explore their association with their host galaxies.

Deliverables expected in the period are:

- List of science papers #1 (D5.1)

5.2 Results from first year.

Due to the inevitable gestation period, science papers that have genuinely benefitted from ASTRODEEP funding have only been completed and submitted towards the end of 2013. Nevertheless, we can already report on 6 refereed journal papers that have now been submitted for publication. These papers all present significant scientific advances based on early versions of catalogues within the key survey fields that are the focus of the ASTODEEP project. In several cases the analysis undertaken en route to science results has revealed both the strengths and deficiencies of existing catalogues, reaffirming the central premise of ASTRODEEP that high-quality data products can only be produced and validated in conjunction with cutting-edge research. Below we provide a brief summary of the key results from each of these papers, describing in each case the status of the new datasets from which they were derived.

Bowler, Dunlop et al., 2013, MNRAS, submitted (arXiv:1312.5643)
"The bright end of the galaxy luminosity function at z ~ 7: before the onset of mass quenching?"
This paper presents the first science results based on the second data release (DR2) of the UltraVISTA survey, and the latest (DR10) release from the UKIDSS UDS survey. These two surveys are providing the key near-infrared imaging across the two largest (degree-scale) fields to be analysed within the ASTRODEEP project. However, the proper exploitation of these data in the study of high-redshift galaxies requires that they be combined in a resolution-matched way with optical (Subaru and CFHT) and mid-infrared (Spitzer) data. In this study a first version of such a combined multi-wavelength catalogue has been used to produce a new sample of ~35 luminous galaxies at redshift z ~ 7. The most important result is that such galaxies appear to be more numerous than expected based on the standard (Schecter function) extrapolation from the number density of fainter z ~ 7 galaxies (as revealed by smaller-area deeper surveys with HST). Interestingly, this suggests the form of the bright–end of the galaxy luminosity function at z ~7 simply mirrors the high-mass end of the dark-matter halo mass function, and hence that the physical mechanism which produces the very steep decline in the number of luminous galaxies seen in the low-redshift Universe has yet to impact on the galaxy population at z ~7 (within the first billion years of cosmic time). While undertaking the analysis reported in this paper, a problem was uncovered with the calibration of the UltraVISTA DR1 Y-band data, and this has now been corrected in DR2 (once again emphasizing the importance of catalogue production proceeding in parallel with scientific validation).

Rogers, McLure, Dunlop et al., 2013, MNRAS, submitted (arXiv:1312.4975)
"The colour distribution of galaxies at redshift five"

This paper presents new results on the colours of high-redshift galaxies, this time at z~5, where the higher signal-noise and additional rest-frame coverage of the galaxy spectral energy distributions enables more detailed study of the controversial issue of the galaxy colour-magnitude relation (CMR) than at higher redshifts. Crucially, in order to achieve maximum dynamic range in luminosity, this work relies on combining ground-based and space-based (HST) imaging, a key focus of AstroDEEP. The galaxy samples and the associated galaxy photometry was derived from the HUDF12 imaging in the Hubble Ultra Deep Field, the HST CANDELS imaging in the GOODS North and South fields, and the ground-based imaging in the UKIDSS UDS field. The paper presents two key results. First, it reaffirms and clarifies the form of the colour-magnitude relation at z~5. Second, it presents the first statistically-significant evidence for a scatter in intrinsic colour at the redshifts, a variation which appears to increase with increasing UV luminosity. The conclusion is that the increasing width of the intrinsic galaxy colour distribution and the CMR itself are both plausibly explained by a luminosity independent lower limit on UV slope, combined with an increase in the fraction of red galaxies with increasing UV luminosity.

Castellano, Sommariva, Fontana et al. 2013, A&A, submitted
"Constraints on the star-formation rate of z~3 LBGs with measured metallicity in the CANDELS GOODS-South field"
This paper is focused on the properties of galaxies at somewhat lower redshift, at z~3 which corresponds to the peak epoch of star-formation activity in the Universe. The paper exploits the latest photometry in the GOODS South field to enable detailed fitting of the spectral energy distributions (SEDs) of a subset of z~3 galaxies which possess spectroscopic redshifts. The power of this approach is that the spectroscopy not only provides the reassurance of accurate redshifts, but also helps to break some the degeneracies which often plague the extraction of robust physical parameters from SED fitting based purely on photometry. One key conclusion is confirmation that the appropriate metallicity to use in the fitting is ~0.1 times the solar value. Adopting this metallicity, and then fitting a range of star-formation histories to the combined optical-infrared photometry, yields star-formation rates for these objects which suggest that the star-formation density at z~3 is even higher than previously thought. We note that this paper also makes use of the new near-infrared data in the GOODS-South field provided by members of our team through the VLT Hawk-I HUGS program, and thus provides another example of the importance of coherently combining ground-based and space-based data.

Sommariva, Fontana et al., 2013, A&A, submitted
"A mass threshold in the number density of passive galaxies at z~2"
This paper again utilizes the new HUGS K-band data in tandem with existing HST and ground-based data, but this time in both the GOODS-South and UDS fields, and in the study of passive galaxies at redshifts z~2. Once again the importance of properly matching the space-based and ground-based photometry is emphasized, as here use is made of well-established BzK colour-criteria to select galaxies at z ~2 in which star-formation activity has been quenched. The key breakthrough enabled here is that, by extending the study of BzK selected passive galaxies a magnitude fainter than was previously possible, this work has revealed a clear turnover in the number density of quiescent galaxies below a stellar mass threshold of $M^* \sim 10^{10.8}$ solar masses. This result confirms (and better quantifies) previous suggestions that passive galaxies are confined to the high-mass regime at these redshifts, and comparison with the predictions of various current models of galaxy formation shows that none of them can properly reproduce this key feature of the evolving galaxy population. This work thus

demonstrates that the evolving mass function of passive galaxies continues to present one of the key challenges for proposed models of galaxy formation and evolution.

Fontana, Dunlop et al., 2013, A&A, submitted
"The Hawk-I UDS and GOODS Survey (HUGS): Survey Design and Deep K-band Number Counts"
This paper presents the survey design of the near-infrared Hawk-I UDS and GOODS Survey (HUGS) that was utilized in the afore-mentioned two studies. It also exploits these new, deepest-ever K-band data to explore the K-band galaxy number counts to previously unexplored depths. This is a crucial dataset for many studies of distant galaxies because HST is not capable of imaging at wavelengths longer than 1.6 microns. By providing deep, high-quality (0.4 arcsec seeing) imaging at 2.2 microns, HUGS fills a crucial gap in spectral coverage between the HST and Spitzer data in two of the CANDELS survey fields. This paper demonstrates that the HUGS K-band data are well-matched in depth to the CANDELS HST H-band imaging, validating the approach taken in designing the survey. It also shows that the slope of the deep K-band galaxy number counts depends sensitively on the assumed distribution of galaxy sizes, with potential impact on the estimated extra-galactic background light

Vanzella, Fontana et al., 2013, ApJ, 2013, submitted
"LBT/MODS1 spectroscopic confirmation of two faint sources at z=6.4 magnified by the CLASH / Frontier Fields cluster MACSJ0717.5+3745: towards the characterization of star-forming galaxies at the epoch of reionization"
This paper presents some of the very first results from analysis of the first HST Frontier Fields dataset. Specifically, the paper presents spectroscopic results from the Large Binocular Telescope which show that two of the faint galaxies gravitationally lensed by the galaxy cluster MACS0717.5+3745 lie at redshift z = 6.4. This redshift information, in tandem with the deep multi-wavelength HST imaging enables study of the SEDs of two faint z~6.4 galaxies, galaxies which have lower luminosities than those which can be studied without the aid of gravitational lensing. These galaxies are, as expected, compact and of low stellar mass. However, perhaps the most interesting finding is that they seem to be extremely blue, displaying a UV continuum shape that appears to reflect the presence of extremely young and extremely low metallicity stellar populations.

6. WP6: Simulations of the Euclid deep survey

This WP builds on the expertise gained in the other WPs to prepare the tools in preparation of the EUCLID Deep survey. The whole WP will start later, in Year 3, in order that it can be built on the foundation of the results of other WPs.
No reporting is due at this period.

7. WP7: Dissemination and Outreach

7.1 Description and goals of WP7

The main objective of this WP is to distribute to the community the output from the ASTRODEEP project. This will be achieved though the creation of a unified portal for data access, publications to scientific journals of all main results and the organization of at least one major scientific conference focused on the topics studied within the project.

Deliverables expected in the period are:

- Beta release of public web portal (D7.1) (Delivered)
- Public release of public web portal (D7.2) (Delayed – expected delivery March 2014)
- Call for collaboration meeting (D7.3) (Delivered)

7.2 The development of the ASTRODEEP web portal

The main activity in this period is related to the development of a web portal.

First, we have created, and made accessible, a web-site that describes the ASTRODEEP project. This web site has been designed with a simple Web editor and put online relatively early in 2014.

Next we have undertaken the design of the final Web portal that will be used to fully document and release our software, catalogues and scientific papers, as well as the outreach material for the general public. Our main aim is to produce a service provider for the professional audience, offering well-documented access to our tools and products.
However, the website is also designed to be used as an internal collaboration tool, to share documents and other information between the various ASTRODEEP participants and affiliates.

The design and realization of the web portal has been sub-contracted to a professional web designer. The project has been formulated and presented, and is currently being implemented.

The design and realization of the portal has been somewhat slowed down with respect to the original plan essentially because of a delay in the preparation of the requirements and of administrative delays in placing the relevant contract with the external web designer. We already have a working site that we plan to finalize in January and show during the review meeting.

7.3 The consortium meeting

One of the main goals of ASTRODEEP is to broaden the collaboration between the main teams that are active in Europe in the exploitation of the deepest images of the Universe.
At this purpose, well-focused scientific meetings are crucial to establish connections, foster new ideas, and spread latest ideas and news among the scientists.
In this context, we proposed to organize a scientific meeting focused to gather the participants of the CANDELS and GOODS-HERSCHEL surveys to discuss a well defined scientific aspect.

We decided to organize the meeting entitled "**The Spectral Energy Distribution of high redshift galaxies: lessons learned and open questions".**
It will be held at the Sexten Center for Astrophysics (Sesto Val Pusteria, Italy) in January 2015.

We decided to organize the meeting in January 2015, slightly later than originally planned in the DoW (second year). This choice has been taken after considering the planned date of release of the main datasets (including the ASTRODEEP-released catalogs) for the

forthcoming new generation of surveys: the full CANDELS data set (mid 2014), the HERSCHEL-CANDELS data set (August 2014), the ALMA deep field (mid-2014), the first set of the Frontier Fields(late 2014). Taking into account that a proper analysis of these data sets requires at least some month, a meeting in January 2015 seems to guarantee the optimal timing for an appropriate scientific discussion of the results from these surveys.

Full scientific rationale and more details can be found in D7.3.
It is already announced in the web page of the Sexten Center: http://www.sexten-cfa.eu/

8. Project management during this period

8.1 WP1: Management

Deliverables expected in this period:

- Methodology of the emission of the calls for external consultants – D1.1 and MS6 – **delivered**

8.1.1 General activities

The ASTRODEEP Consortium includes 4 partner institutes (INAF, UEDIN, CEA, CNRS) and one third-party, the University of Strasburg, connected to CNRS. The co-ordination of the project is led by INAF in close collaboration with the Executive Committee (EC) that includes:

- Adriano Fontana, Coordinator (INAF – OA Rome, I)
- James Dunlop (University of Edinburgh, UK)
- David Elbaz (CEA-Saclay, FR)
- S. Derriere (CDS Strasbourg, FR)
- A. Comastri (INAF – OA Bologna, I)
- S. Faber (Univ. of S. Cruz, USA)
- H. Ferguson (STScI, USA)

In December 2012 all partners signed the Consortium Agreement (CA), where internal rules are described. REA was notified of this action and the Grant Agreement was officially signed by REA on 27/12/2012. The official starting date of the project is: 01/01/2013.

The coordinator has received a total pre-financing sum of 951.543,17eu, which has been distributed among partners, according to the following table:

Guarantee Fund	95154.31eu
INAF	326337.0eu
UEDIN	260277.9eu
CEA	225351.75eu
CNRS	44422.2eu

In April 2013, we received from REA a request for an amendment to the Grant Agreement in order to align the existing GA to the revised Financial Regulations. Such action introduces the electronic-only submission of the financial statements (FormC) and the certificates on financial statements and certificates on methodology (FormD and E). Following the procedure suggested by the REA, a formal amendment request was presented and was accepted on October 4th, 2013. The amendment takes effect from 01/01/2014.

8.1.2 New personnel

Within the framework of the project, a number of post-doctoral research associates (PDRA) have been hired to participate in the scientific activities, associated to the following task over the next two-three years:

- Ricardo Amorin (INAF-OAR): Galaxy evolution, rest-frame properties of galaxies at high redshift, in particular faint galaxies of low metallicity (WP5); Data analysis and catalog production (WP4).
- Emilian Merlin (INAF-OAR). Development and testing of dedicated software for photometric analysis, in particular at the optical-near IR domain. Analysis and refinement of TFIT and CONVPHOT (WP3); Catalog production (WP4); SED of high redshift galaxies and comparison with theoretical models of galaxy formation (WP5).
- Nico Cappelluti (INAF-OABo). Analysis of X-ray survey over CANDELS fields, with a special emphasis on the 4Ms Chandra survey on the GOODS-S field.
- Nathan Bourne (UEDIN). Identification of SMG counterparts in Herschel-ATLAS survey; far-IR properties of high redshift galaxies (WP5)
- Victoria Bruce (UEDIN) Morphology of high redshift galaxies (WP5); use of morphological parameters for accurate photometry of faint galaxies (WP3)
- Xinwen Shu (CEA) Advanced methods of detection in Herschel images (WP3). Properties of high redshift dusty galaxies (WP5)
- Tao Wang (CEA) Simulations of deep Herschel fields; prior photometry in Herschel data (WP3). Star Formation in high redshift galaxies (WP5).

Konstantina Boutsia has been hired for keeping track of management issues of the project (WP1) and for keeping updated the project websites (both preliminary ones and the official one that is currently under construction). According to her contract she spends 67% of her time working for Astrodeep and 33% working for the ERC –FIRST project. She was hired in August which amount to 3.3p/m dedicated to the project of which 1p/m in WP1 and 2.3p/m to WP7 and WP2.

The selection of the PDRAs has been done through international calls, posted on the most diffused web site of job advertisement in astronomy (AAS Job register).

1) INAF-OAR opened two calls, one more science-oriented and one more technologically oriented

The science oriented collected 30 different applications, 12 of which of male gender. Of these, 9 (3 males) were shortlisted and interviewed. 8 of them declined their interest before the selection was completed (due to unforeseen delay in the selection process) and the final selected applicant is Ricardo Amorin.

For the software-oriented call, 11 application were received (8 males). There was no shortlist done, since Emiliano Merlin clearly stood out as the best candidate, and was directly appointed.

INAF-OABo opened a scientific oriented position which collected 7 applications altogether (3 males). Two of them (both female) could not be considered because arrived after the deadline and so the final number of valid applications was 5. There was no shortlist, since

Nico Cappelluti, clearly emerged as the best candidate on the basis of his curriculum and was directly appointed.

2) UEDIN made a single call for two positions. Out of 39 applicants, 12 were of female gender. 12 were interviewed, 5 of which were women. Two were eventually appointed: Nathan Bourne and Victoria Bruce.

3) CEA made a single call for two positions. Received 57 applications, out of which 22 were women. 18 were shortlisted, including 8 women. On the basis of their technical expertiese Xinwen Shu and Tao Wang (both male) were eventually selected.

8.1.3 External consultants

A number of visiting scientists also participated in the project's scientific activity, using the resources specifically allocated for "external consultants". This programme has been implemented to enhance collaboration between members of the consortium and international scientists for an efficient exchange of expertise and data connected to the main scientific goals of ASTRODEEP. Under this WP a deliverable was foreseen that should describe in detail the methodology for the emission of the calls for scientific consultants. This document includes a description of potential applicants, the timeframe of the various calls, the selection procedures, and the text of the actual call that is emitted periodically by the consortium.

For the year 2013, five external consultants have been granted funding for short and medium term stays in the beneficiary institutes:

- Kuang-Han Huang : 25/05-01/06/2013 at INAF-OAR
- Ashish Ganta: 20/05 – 23/07/2013 at INAF-OAR
- Neil Nagar : 20/09 – 20/10/2013 at CEA
- Roger Leiton : 09/09 – 11/10/2013 at CEA
- Jonathan Trump: 03/12 – 07/12/2013 at UEDIN

8.2 WP2: Scientific Management

To permit smooth coordination between the various partners and to achieve an efficient collaboration various methods have been utilised.

Two mailing lists were created, one including only the members of the EC (astrodeep-ec<at>oa-roma.inaf.it), for strictly administrative matters, and one including all people involved with the Astrodeep project (astrodeep-all<at>oa-roma.inaf.it), for scientific collaboration. Mails are regularly used for communication among all participants.

An online management tool, called "basecamp" is used for the exchange of material and comments on on-going projects. Using this software we may create "to-do" lists shared among all participants or, when necessary, with particular working groups. This is an efficient way of tracking which tasks are assigned to whom, progress and completeness, and the various deadlines. An additional advantage of such management tools is that all material is available online to everyone, discussions are easily browsed and the history of a single task can be reconstructed swiftly and thoroughly, without the risk of losing information along the way.

This tool has been implemented during the last two months and after a successful trial period we expect to use it regularly for communication and task assignment for the remaining of the project. This is a variation with respect to the management tool mentioned in the deliverable D2.1, since at the beginning we were using "Smartsheet" which has recently been abandoned.

List of project meetings:

In the first twelve months of the project two meetings have been organized:

- ***Kick –Off Meeting***: Sesto in Pusteria (Italy) – 29-30 Jan. 2013
  This meeting was the first one to take place after the beginning of the project.
  Most of the EC was present, as well as a few of the post-doctoral associates that would likely be involved in the project. During this meeting we discussed the main goals of the project, first deliverables and milestones, and laid out the plan of main activities.

- ***First collaboration meeting***: IAP in Paris (France) – 24-25 Jun. 2013
  Once the hiring procedures were finalized, a second meeting took place in Paris (CEA-Saclay) to give a chance for all members to get acquainted and present their work and expertise. During this meeting a more detailed work plan was established, so that all activities due to produce deliverables in this period would be completed in time.

- ***Telecons:***
  In the second meeting it was decided to have regular telecons in order to better coordinate and keep track of all activities. In this first year, three telecons took place:
  Oct. 3, 2013
  Nov. 7, 2013
  Dec. 3, 2013

Other trips

During this first period a limited number of trips were funded by the Astrodeep project.

- Henry Ferguson (EC member) has joined the two external consultants at INAF-OAR during the week of 25/05-01/06/2013. Since he is directly involved in the development of the various codes used by the project, he provided useful insight and helped maximize the outcome of these collaborations.
- Emiliano Merlin spent two weeks (2-13 dec 2013) at STScI in Balitmore to work with H. Ferguson on the development of the version of TFIT;
- Adriano Fontana spent one day (13 November 2012) at CEA in a meeting dedicated to the review of the work on the Herschel images; This trip was not funded by ASTRODEEP.
- Adriano Fontana spent 4 days in Baltimore (9-12 dec 2013) to work with H. Ferguson and E. Merlin (in visit, as described above). This trip was not funded by ASTRODEEP.
- In September 2013, Andrea Comastri and Nico Cappelluti have participated at 3rd XMM-CDFS meeting (Athens, September 2013), where they presented preliminary results on the X-ray dataset used by Astrodeep. Subsequently Andrea Comastri presented preliminary results on X-ray catalogs created for the Astrodeep project as an invited speaker at the conference: "Explosive Transients: Lighthouses of the Universe" (Santorini, September 2013).

Project planning and status:
All deliverables expected for this period have been presented and the project is on track.

Impact of possible deviations from the planned milestones:
No deviations from the planned milestones have been necessary for this period. The foreseen milestones in the first twelve months are detailed below:
MS6 – Internal Call – Methodology for emission of the call for scientific consultants – month 4 – delivered
MS7 – Management Portal – month 6 – delivered
MS8 – First list of science papers – month 12 – will be delivered

Changes to the legal status of any of the beneficiaries:
To our knowledge there have been no changes to the legal status of the beneficiaries.

Development of the ASTRODEEP website:

This first year the ASTRODEEP website has been under development, thus undergoing frequent changes, updates and upgrades. The first "beta" version of the site has been presented in the deliverable D7.1. That version has since been replaced by a new site created in a WordPress environment. An external web-designer has been *sub-contracted*, since resources for this task were included in the official budget.

The new ASTRODEEP website includes four main sections that present the main activity areas of the project: Science, Data, Software and Outreach. This new site is particularly oriented to an expert audience (professional astronomers) with the "Outreach" section including also material suitable for the wider public. All scientific products of the project (e.g. new software, scientific sky images and simulations, catalogues, scientific publications) will be available through the website. On the section "project" we have made available all Work Packages foreseen by the DoW along with all related deliverables for public consultation.

Problems and how they were solved:
No significant problems were encountered in this period.

9. Appendices

9.1 Addendum to 3.2.1: Toward a new generation of TFIT

We started our investigation by comparing the main features and the performance of the two tools used at INAF Rome, namely TFIT (Laidler et al. 2007, PASP, 119, 1325) and CONVPHOT (De Santis et al. 2006, NewA, 12 271). Both of these are designed to perform PSF-matched photometry on low-resolution images using a high-resolution image as a prior for the positions and structures of the objects (for more details on the codes, see the Scientific Software Report). Then, in order to better identify and ultimately eliminate the obscure differences found between the outputs of these routines, E. Merlin developed a new software package, named T-PHOT, which combines the two and improves upon their weak points. Its aim is to obtain a robust and easy-to-handle main code, with a clear structural architecture (namely, stemming from the state-of-the-art TFIT, a Python envelope calling C/C++ codes which actually "do the job", but reducing Python workload in favour of faster C modules), in which different routines for various numerical/conceptual methods are implemented, and can be selected using simple switches. The goal is to test which key routines within the code perform best and produce the most robust results under different circumstances. Also, T-PHOT is designed to be a more stand-alone software package than TFIT, requiring only CFITSIO and FFTW3 libraries as external software, plus of course a few Python modules.
In the long term, our plan is that the different options currently available will be frozen shall into a "best-choice" default parameter set (based on the results of our testing), and the user will be free to choose whether to use T-PHOT in this standard setup, or alternatively their own set of preferred parameters.

T-PHOT in its present form has been developed by E. Merlin in the period June-October 2013. It is now ready to be (and it already is being) used as a powerful tool for a systematic investigation of the pros and cons of each single procedure, in a very straightforward way.
A detailed comparison between the results of TFIT, CONVPHOT and T-PHOT is being performed, to ensure the equivalence of the results when the settings should require it, and/or understand the causes of possible differences.
Moreover, a systematic survey of the capabilities and results of the many possible combinations of different methods is being performed using T-PHOT, with the aid of an extended set of simulated images obtained using the SkyMaker software package (Bertin) and a specific purpose-built Python script written by E. Merlin in collaboration with A. Grazian and M. Castellano (see below).

The first important result obtained with T-PHOT is a massive saving of computational time and of RAM memory both with respect to TFIT and CONVPHOT.
For example, a complete, double-pass run on the whole UDS field at once (ca. 35000 sources; LRI 30720x12800 = 400 millions pixels; standard TFIT parameters, FFT convolution) is completed without memory swaps in ca. 2 hours (1 hour for the first pass and 1 hour for the second pass). A complete, double pass run on the Goods-South Hawk-I W1 field (17460 sources, LRI 10700x10600 = 100 millions pixels, identical parameter space as for UDS) is completed in ca. 20 minutes.
For comparison, TFIT requires many hours (ca. 24) to complete a single pass on the Hawk-I field. It must be said that TFIT by default produces cutouts and templates for *all* the sources in the HRI images; selecting the ones belonging to the LRI field and inputting an ad-hoc catalog would have reduced the computing time, say by a factor of two (i.e., 11 hours for the a single pass). It was not possible to process large images like the UDS field in a single run, because of

RAM memory failing.
CONVPHOT timings and memory problems are similar to those encountered with TFIT ones, albeit generally for different reasons (being written in C, it is generally faster, but it employs a slower convolution method and the solution of the linear system is much more time consuming, as it is performed via a single large matrix inversion instead of dividing the image in cells as is done with TFIT).
The large saving of computational time in T-PHOT (tens to hundreds of times faster) can therefore be attributed to three distinct factors: 1) the substitution of TFIT Python scripts (high-level, interpreted language) with C codes (low level, compiled language); 2) the Fast Fourier Transform (FFT) method (which was already implemented in TFIT but not in CONVPHOT) in the hi-res cutouts convolution procedure; 3) the cell-fitting method (in which the image is divided into cells which are fitted separately), which allows the fitting of large images in a relatively short time compared with the whole-image-at-once approach (the latter being the method adopted in CONVPHOT).

Coming to the scientific and technical scope, we here provide a brief summary of the methods checked so far, and of the preliminary results of this survey following the original TFIT processing flow:

- Cutout stage. In this stage, each source detected in the high-resolution image (as reported in the SExtractor catalog) is cut out and stored in a fits thumbnail. In TFIT this was performed using a Python module that calls an IRAF task. In T-PHOT this has been replaced with a C module. Also, this stage can now be skipped if desired, as cut-outs can be retailed directly during the subsequent convolution stage.
- Convolution stage. Here each cut-out is convolved with the convolution kernel to obtain a low-resolution model. In CONVPHOT this is performed via straightforward pixel convolution, while in TFIT a call to the Python module *anfft* allows for a FFT convolution. In T-PHOT both solutions are possible; the FFT method is much faster. The convolution is performed using a C module.
- Cull stage. In TFIT, once *all* sources have been convolved, they are checked one by one to see which ones are really inside the low resolution field. Of course, this might result in a (large) waste of time. In T-PHOT this check is performed *before* convolving the high resolution cut-outs.
- Fitting stage. The TFIT C++ core code is still used, but it has been upgraded to include many of the specific CONVPHOT recipes and also new possibilities. These include: whole image fitting; three different methods of matrix solving (namely, LU, Cholesky and Iterative Biconjugate Gradient Method); fitting limited to the central regions of the templates, to avoid PSF wings contamination; clipping out of negative sources; cells centered on single objects instead of arbitrary grid.

Noticeably, fitting on single cells as done in TFIT can lead to potentially large errors, because of the exclusion of nearby and potentially contaminating sources from the cell being fitted. Since the whole image fitting approach needs large amounts of computational time, a method to cure this problem should be identified and implemented. E. Merlin is currently working on this key issue, testing different approaches to decide if and when an object might be excluded from a cell without leading to non-negligible errors.

- Dance stage. In TFIT, after the first fit a complete re-registration of the convolution kernel is performed, dividing the measurement image into regions in which the shifts are computed by means of a local cross-correlation between the real image and a synthetic image produced using a collage of the model templates. This is achieved calling two IRAF tasks via Python modules. In T-PHOT, all of this is accomplished using

a C module.

An extended set of simulations is currently being produced and investigated, including synthetic images and manipulated real images. The aim of the task is to make extensive comparisons between different approaches, both in terms of reliability of the results and of computational performance, highlighting weak-points and limits.

The main goals of the simulations task are:
(a) Validation of different numerical methods. Some examples are:

- many cells vs. single cell fitting;
- different matrix solvers (LU and Cholesky decomposition, Iterative Biconjugate Gradient method);
- inclusion of a threshold on the flux to be fitted;
- clipping out of negative flux sources;
- possible different kernel registration methods.

(b) Validation of the error budget determination. Are errors estimated correctly? Is the covariance of each source the best way to estimate its uncertainties?

(c) Highlighting correlations in the parameter field, if any. For example: Δf (expected vs. measured) vs. blending, separation, etc.

(d) Finally, at least as a long term goal, studies and tests should be performed to assess the impact of such complicating factors as differences in flux at varying the wavelength (colors), changes in morphology with wavelength, astrometry problems, etc.

All of the tests should evaluate the performance of the algorithms in terms of numerical stability, reliability of the results, and computational speed.

Among the different possibilities for the software to be used to prepare the simulated images, we choose to use the software tool *SkyMaker* developed by Emmanuel Bertin & Pascal Fouqué (Bertin 2009, MmSAI, 80, 422B; http://www.astromatic.net/software/skymaker). *SkyMaker* is a public software package distributed under the GNU license. It builds synthetic images starting from an input catalogue (in ASCII format) to be prepared a priori, which may include stars and galaxies with any desired positions, magnitudes and shapes, and simulates the observational properties of a real observing facility when provided with input values of the relevant parameters (e.g. FWHM, pixel scale, diameter of primary and secondary mirrors, gain, saturation level, exposure time, zero point, background magnitude, etc.). Furthermore, the same input catalogue can be transformed into images at different resolutions by the code itself, just through changing the parameters of the "synthetic telescope", thus mimicking the desired effect without the need to artificially blur the high-resolution image a posteriori, and obtaining consistent, registered images with the same pixel-scale.
Using *SkyMaker,* good control of the properties of the synthetic objects (positions and magnitudes) and on the characteristics of the simulated observation process is ensured. Therefore, attention can be focused purely on the photometry task. In particular, it may be interesting to check how the usage of standard software to obtain priors (e.g. Bertin's SExtractor) may affect the final results given different segmentation maps.

E. Merlin has developed a Python script to make the process of generating synthetic images (total, normalized to 1s exposure time, background or noise subtracted; both high and low-

resolution), segmentations, PSF, input and output catalogues with *SkyMaker* automatic and user-friendly.

The task is subdivided into different steps.
0-A) Simulation and analysis of a set of small synthetic images, each containing two extended objects (galaxies), displaced at different relative distances implying different levels of blending, and/or having different magnitudes; the low-resolution version of the same image (obtained by degrading the high resolution one) may be replicated with different realizations of the background noise. Goals: to check the reliability of each code in this very basic task, ensuring the validity of the standard methods, measuring Δf (expected vs. measured); to check for correlations of the results with the varying parameters (separation, input Δf); to check the detection limits; and to analyze the error budget estimation in relation to the varying noise realizations.
0-B) Simulation and analysis of a set of small synthetic images, each containing five extended objects (galaxies) displaced in a standard geometrical disposition, displaced at different relative distances, and/or have different magnitudes. Goals: to check the reliability of each code with thorough attention to the case of strong blending of multiple sources, in particular including large differences in relative magnitudes, measuring Δf (expected vs. measured); to check for correlations of the results with the varying parameters (separation, input Δf).
1) Simulation and analysis of a set of a few 2000x3000 pixel fully-synthetic simulated "astronomical" images, containing fake stars and galaxies, displaced according to existing statistics and counts (this is achievable via the *SkyMaker* ancillary code Stuff); the "ideal" HST-like detection images should be degraded to 1.0" (ground-like) and 2.5" (IRAC-like) resolution; no change in fluxes between detection and measure image should be included at this stage (i.e., no colors). Goals: to check the reliability of each code in "real", albeit idealized, situations, measuring Δf (expected vs. measured); to check the detection limits; to check for correlations of the results with the varying parameters (separation, input Δf); and to analyze the error budget estimation in relation to the varying noise realizations.

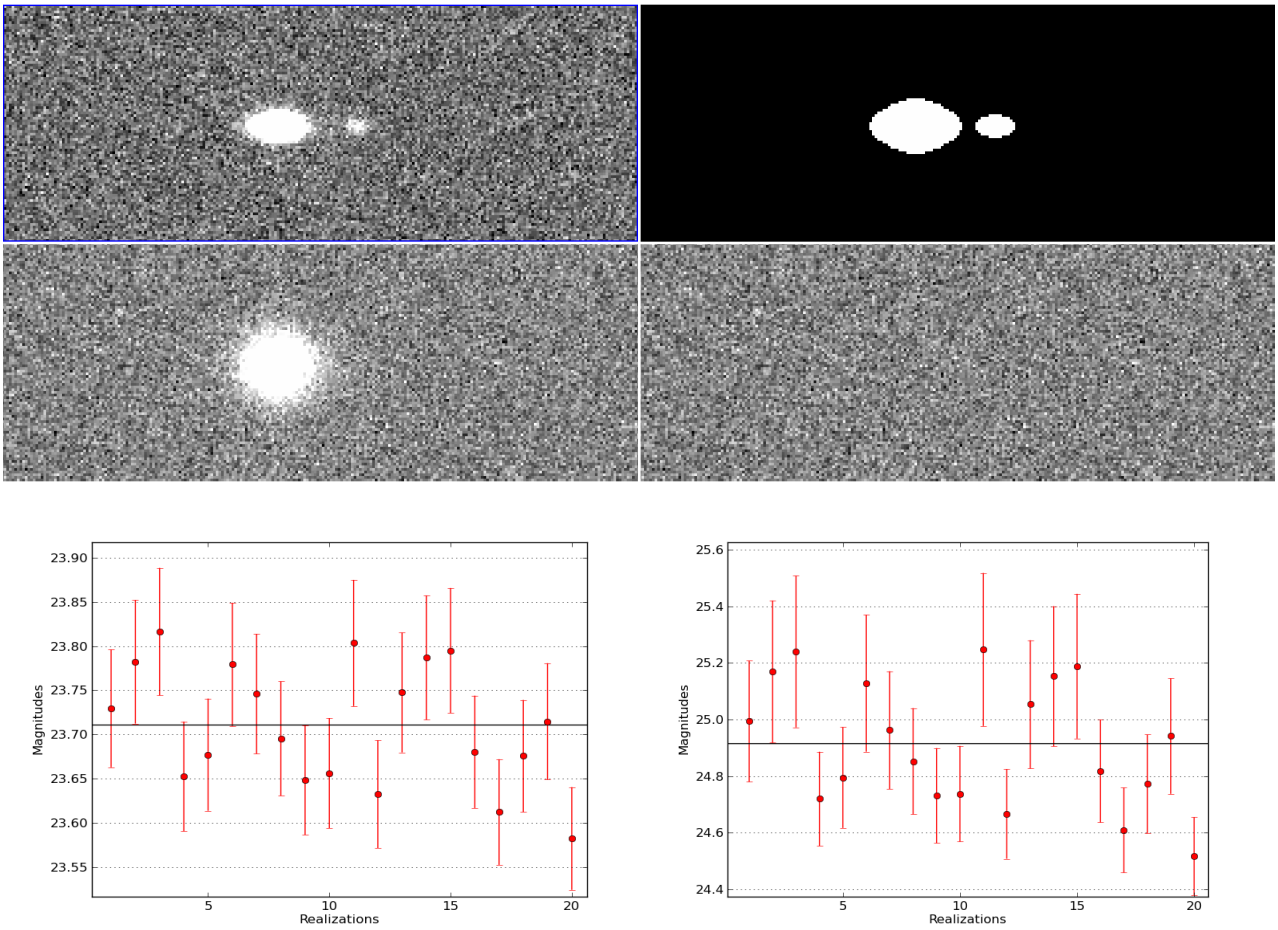


Figure 1 – Example simulation with two objects. Top panel, left to right, top to bottom: detection image (simulated HST F160W image), segmentation map, measurement image (simulating a ground based observation with 1" FWHM), residual image (models subtracted from the measurement image). In this case, the two objects have magnitudes M_1 = 21 and M_2 = 25, with Zero Point = 26 (the fainter object is almost undetectable in the measurement image). Bottom panel: measured magnitude of the fainter object in twenty different noise realizations of the simulation. Left: TFIT with 100x100 pixels cells; right: T-PHOT with single cell fitting. Using the cells approach may lead to large errors (in this case, almost two magnitudes) if the size of the cell is not chosen properly.

2) Same set of images as in the previous step, but changing the relative fluxes when degrading the detection image to lower resolution, thus mimicking the presence of colours. Goal: to analyze the performance and limits of the method in realistic situations, with the presence of flux variations at different wavelengths.
3) Starting from real catalogues and detection images (e.g., CANDELS fields observed with HST, and in particular the UDF in Goods-S), produce degraded measurement images blurring them down to low resolution (this requires the use of additional software, developed by Stefano Pilo & Diego Paris to simulate Euclid observations); no change in fluxes between detection and measurement image should be included at this stage (i.e. no colours). Goal: study of realistic images with real morphologies and displacements.
4) Same set of images as in the previous step, but changing the relative fluxes when degrading the detection image to lower resolution, thus mimicking the presence of colours. Goal: to analyze the performance and limits of the method in realistic situations, including realistic morphologies, counts and displacement, with the presence of flux variations at different wavelengths.

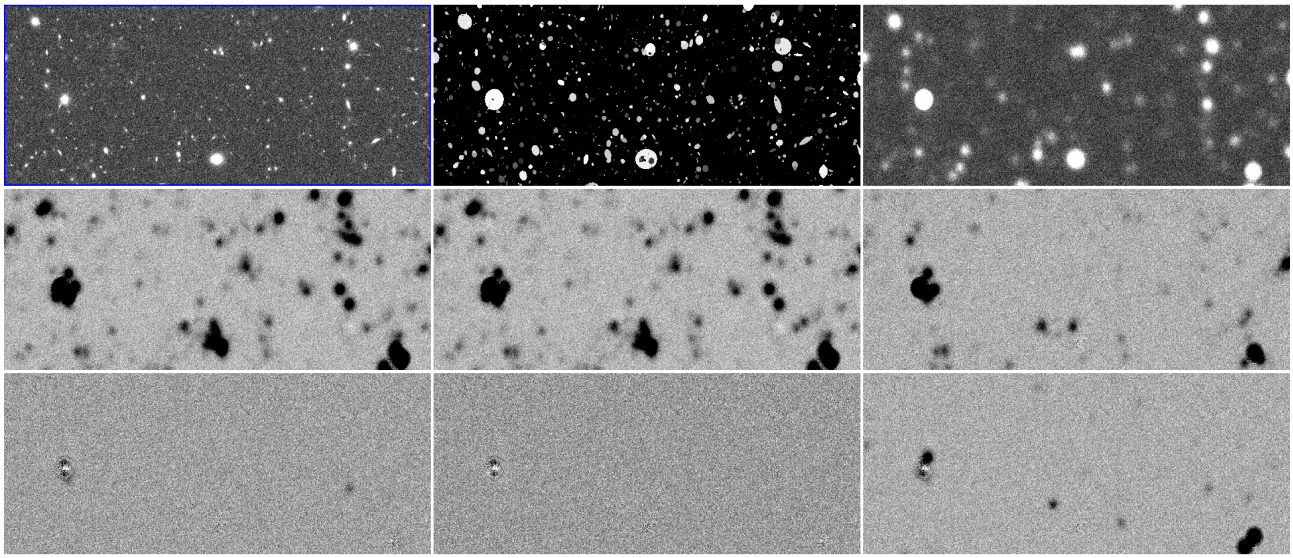


Figure 2 – Simulation of runs with different codes and approaches on the same field. Left to right, top to bottom: high resolution detection image (simulated HST F160W image); segmentation map; low resolution measurement image (simulating an IRAC band-1 image); residual image (models subtracted from the measurement image) obtained with TFIT (cell size: 100x100 pixles); same for T-PHOT with all parameters set as in TFIT (cell size: 100x100 pixels); same for T-PHOT (cell size: 200x200 pixels); same for T-PHOT (single fitting on the whole image); same for CONVPHOT (the difference with T-PHOT is probably due to the clipping out of negative flux sources); same for T-PHOT with cells centered on objects including up to second-order contaminants.

9.2 Addendum to 3.2.2: The analysis of Herschel images

Tuning and testing algorithms for object detection: getsources

We used a simulated *Herschel* image of the GOODS-North field to test the robustness (purity, completeness) of the *getsources* blind multi-wavelength multi-resolution source extraction method. This simulation is one of our suite of mock *Herschel* images produced for each one of the CANDELS fields (GOODS-North, GOODS-South, UDS, COSMOS) which we designed both to test and compare the performance of various source extraction techniques (e.g., prior-based PSF fitting; see next section) and to quantify the impact of the confusion noise in *Herschel* images (e.g. Leiton et al. 2014).

We present here the simultaneous extraction of sources over 6 pass-bands from *Spitzer* MIPS-24μm and *Herschel* PACS-100μm, 160μm to SPIRE-250μm, 350μm and 500μm, using the default configuration of *getsources*. In total 1450 sources are detected with a threshold of 3-sigma above the local background level. Given our knowledge of the input flux densities (S_{in}) of the sources that were used to build the mock images, we can determine the robustness of the flux density measurements with *getsources* (S_{out}) by comparing the difference between both quantities. In the following we will call PAI the *Photometric Accuracy Index* $\Delta S_{out}/S_{out} = (S_{out} - S_{in})/S_{out}$ (as in Magnelli et al. 2009 and Leiton et al. 2014). The PAI ($\Delta S_{out}/S_{out}$) is sensitive to any gain or loss of flux that a source experiences, positive when the flux of the source is overestimated (with a maximum of $\Delta S_{out}/S_{out}=1$) and negative when the source has lost part of its flux to a neighboring source in the extraction process.

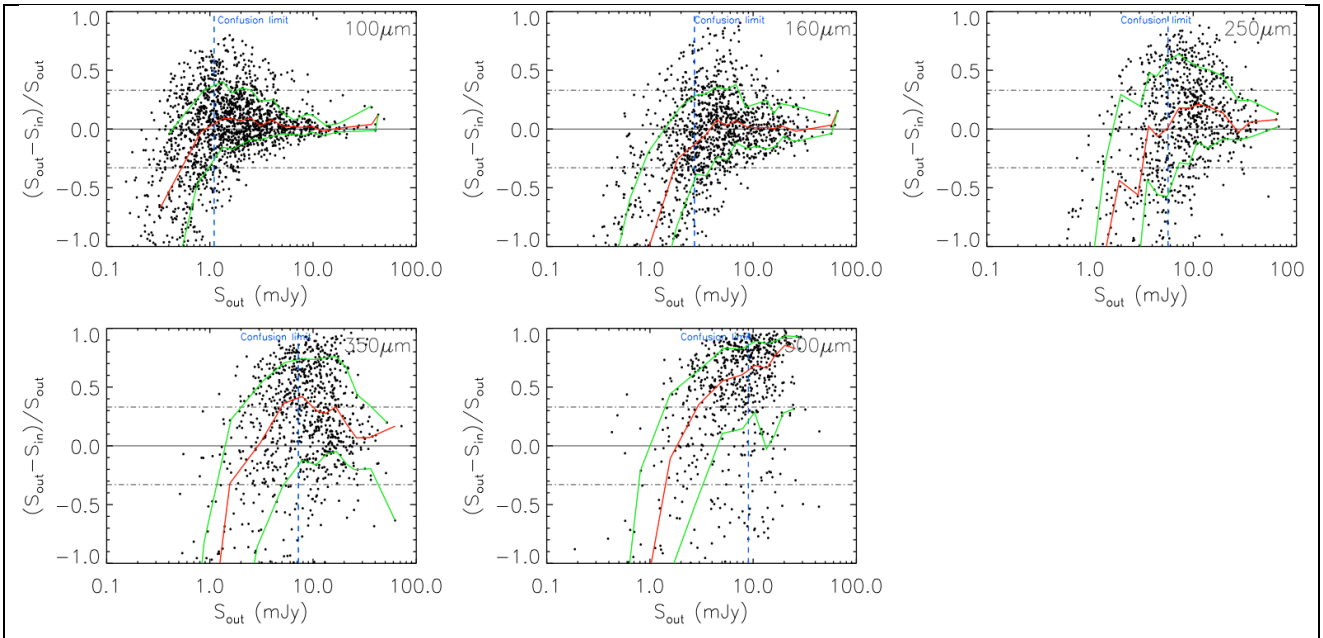


Figure3: Photometric Accuracy Index (PAI), $\Delta S_{out}/S_{out} = (S_{out}-S_{in})/S_{out}$, as a function of the output flux from getsources. The sliding median trend of $\Delta S_{out}/S_{out}$ is shown with a red solid line, while the green lines define the envelope including 68% of the galaxies in a given flux density interval. We define the depth of the catalog by the flux density where the green lines cross the dotted horizontal line marking the $\Delta S_{out}/S_{out} = \pm 0.32$ limit. The resulting vertical blue dashed line is the confusion limit derived by Elbaz et al. (2011), i.e. the depth above which 68% of the sources are detected with an accuracy better than 32%.

Figure 3 shows $\Delta S_{out}/S_{out}$ as a function of S_{out} for the sources matching within 2″ in both catalogues (in total 1305 common sources, orange points). It can be seen that the photometric uncertainty increases inversely with the output flux densities, while smaller $\Delta S_{out}/S_{out}$ means that the flux of the source was accurately extracted by *getsources*. For guidance, two horizontal lines (±0.33) mark the accuracy levels that were used to define the flux limit (dashed vertical line) in the *Herschel* maps (Elbaz et al. 2011). In the PACS 100μm and 160μm bands, at least 68% of the sources can be extracted with an accuracy better than 32% above 1 mJy and 4mJy respectively. This is comparable to the confusion limits derived by Elbaz et al. (2011) in these bands. However, a positive increase in $\Delta S_{out}/S_{out}$ becomes more and more significant in the SPIRE bands with increasing wavelength, suggesting that overestimation of flux densities due to confusion with bright nearby remains a major issue especially at 350 and 500μm.

Comparison between getsources and the standard GOODS PSF-fitting code

Here we present a direct comparison of the performance of *getsources* with the standard 24μm-prior PSF-fitting technique used for the GOODS catalogs. Figure 4shows an example of this comparison for the SPIRE 250μm band. The standard method is more complete above the ~6mJy detection limit and contains less outliers with excess PAI values (purer). The difference is significant even when the parametrization of *getsources* is pushed to deeper levels by lowering by a factor of two the threshold to detect sources during the clean process (cleantuning=0.5) and even though the deeper extraction finds ~70% of the input priors (1852 sources in total, black points in Figure 3 and Figure 4).

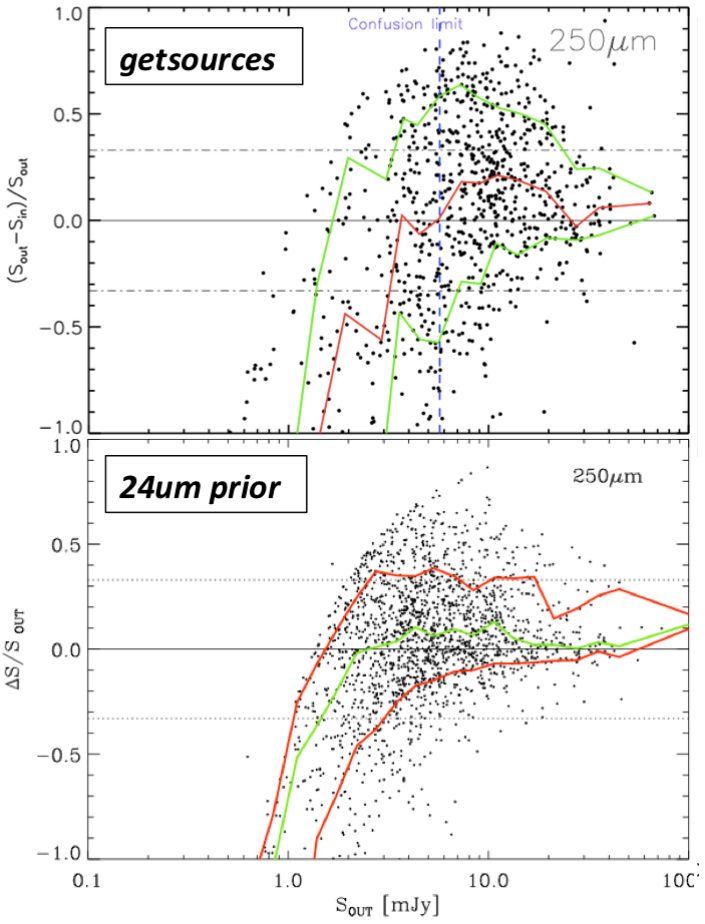


Figure4: Comparison between getsources (upper panel) and 24μm prior technique (bottom panel), at SPIRE-250μm

To estimate completeness and photometric reliability in the output catalog of *getsources,* we plot in Figure 5 the relative fraction of sources with a flux difference less than 32% of their input values (red lines) as a function of *input* flux densities. The completeness is here defined as the fraction of sources detected with a photometric accuracy of better than 32% among *all* input sources which belong to a given flux-density bin. The flux limit where 80% of the input sources are recovered with this photometric accuracy is ~2 mJy, ~6mJy in the PACS 100μm and 160μm bands, while more than 60% of the input sources are recovered above ~10 mJy, ~10mJy, ~25mJy level at SPIRE

250μm, 350μm and 500μm. The latter values are typically a factor of two higher (i.e. shallower) than the ones obtained in the catalogues extracted using 24 μm priors, as we derived in Elbaz et al. (2011). It is actually clear that the catalogues extracted with 24 μm positional priors are deeper than the *getsources* and retrieve more reliable faint sources. In fact at the faint fluxes, spurious sources and confusion start to play a significant role, and the number of sources detected by *getsources* strongly depends on the fine-tuning of the set of parameters, such as detection threshold, measurement threshold, background estimation, source de-blending, photometry, etc., which is currently hard to test without an improvement in the algorithms utilized within the code.

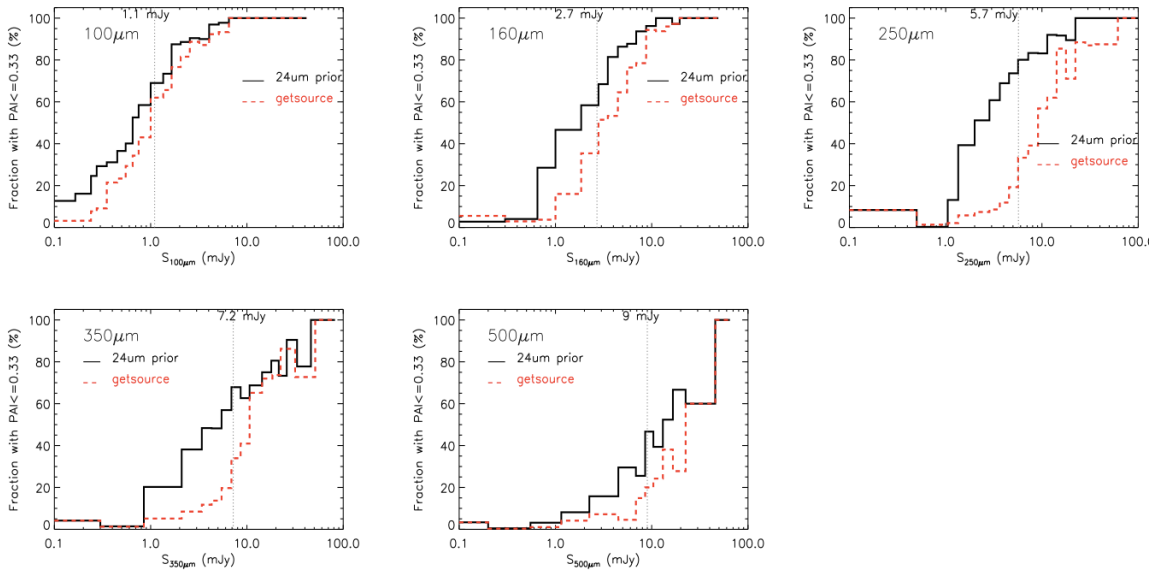


Figure 5: Comparison of the detection rate (or completeness) between getsources and the standard 24μm prior PSF fitting technique as a function of input flux density. Completeness is defined as the fraction of sources detected with a photometric accuracy better than 32% among all input sources within each flux bin.

Future development of getsources

The extensive tests performed on the simulated field have shown that *getsources* was doing a good job in detecting and measuring flux densities *Herschel* sources in the PACS bands, comparable to prior-based PSF-fitting techniques. Although the code loses completeness in the 250-500μm SPIRE bands, it is still useful to perform deep blind source extraction to complement prior-based PSF-fitting techniques which rely on a well defined set of prior positions, e.g. it would be useful to reveal potentially 24μm faint sources below the flux limit of the prior list. Further developments will consist of improving the algorithm of de-blending and background subtraction. The current background subtraction is done by linearly interpolating pixel intensities off the observed image under the segmentation masks based on the pixel values just outside the masks, which strongly depends on the extent of source confusion. One limitation for the source extraction using 24μm priors is the over de-blending of fluxes due to the selection of too many priors, particularly in the SPIRE bands. The blind source list provided by *Getsources* would be helpful to reduce the 24μm priors and improve the Herschel photometry, which will be tested in the future.

Tuning and testing algorithms for PSF-matching:

FASTPHOT

We have tested FASTPHOT on realistic simulated images in the GOODS-North. Details on how the simulated images are produced are present in Leiton et al. (2014). For all priors in the list,

we simulated their far-infrared flux (S_{in}) in all the Herschel bands, and injected them into a realistic noise map. We then ran FASTPHOT on the simulated images, and compare the output flux (S_{out}) to their input flux (S_{in}).

Since the algorithm applied in FASTPHOT to solve the matrix is not bounded to positive solutions, some priors are assigned with negative flux densities. The majority of these priors have very small intrinsic flux in the simulations. We thus run FASTPHOT in an iterative mode; sources with negative output flux are removed in the next run, and are assigned 0 flux in the final catalogue.

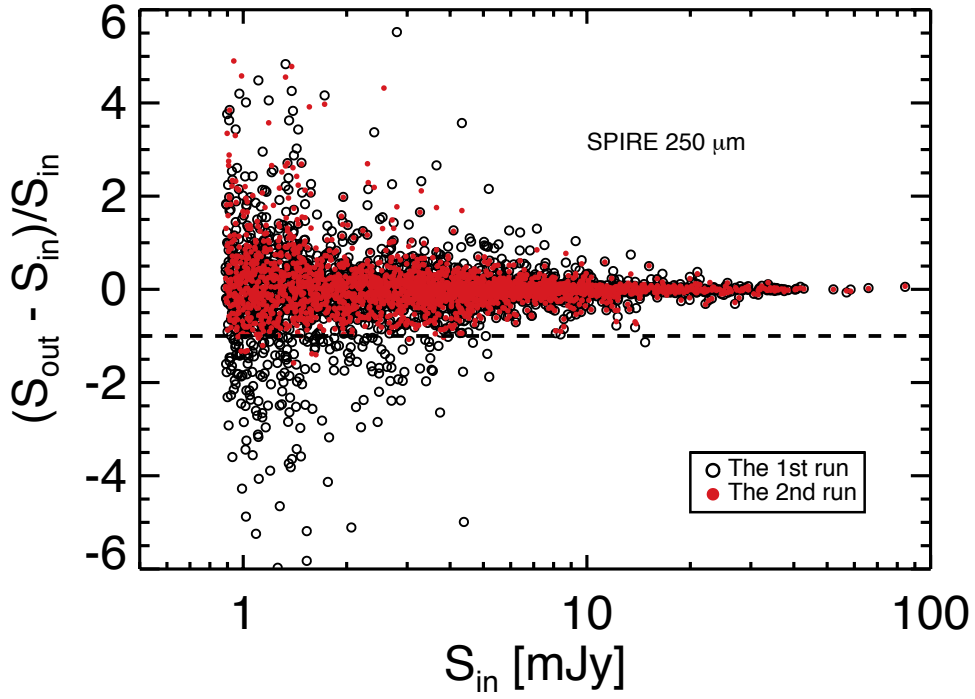
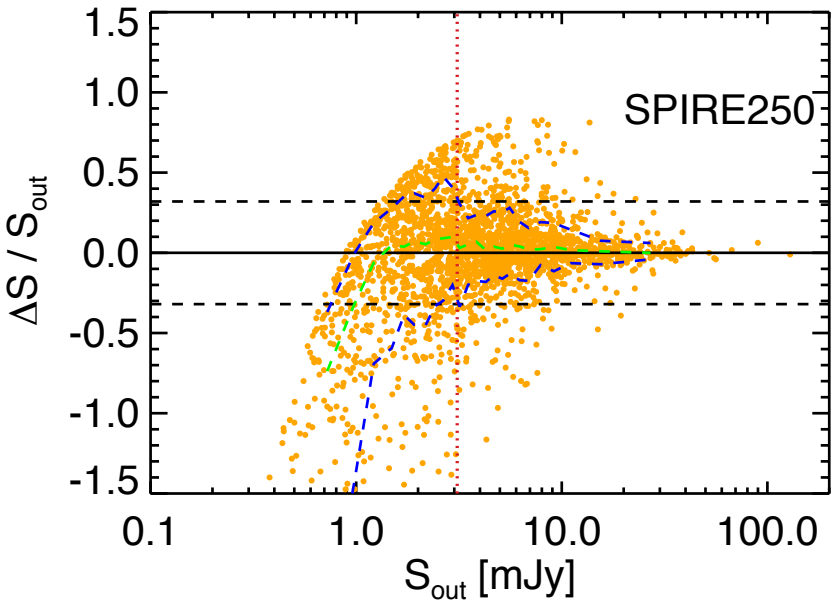


Figure 6: Here we show the comparison between the results from the first and second run of FASTPHOT, taking the SPIRE 250um map as an example. Sources lying below the dashed line have negative flux density ($S_{out} < 0$). In the second run, we remove sources with negative flux densities from the first run from the prior list. Most of the sources with negative flux densities have small intrinsic flux (S_{in}). This also helps to reduce the number of outliers.

To quantify the performance of FASTPHOT, we employ the photometric accuracy index (PAI), $\Delta S/S_{out} = (S_{out} - S_{in})/S_{out}$, as proposed in Leiton et al. (2014). In Figure 7, we show the PAI as a function of the output flux S_{out} at SPIRE 250um.

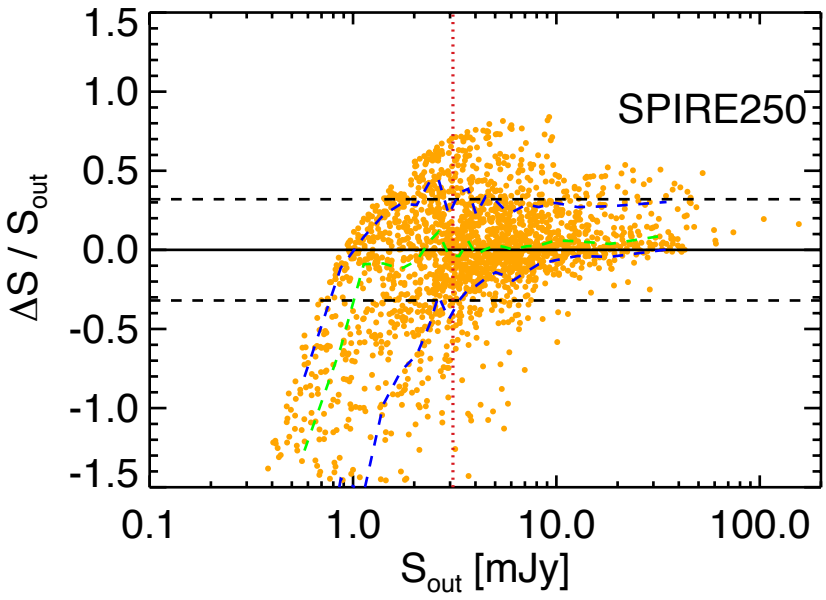


FASTPHOT

Figure 7: Photometric Accuracy index (PAI) as a function of the output flux S_{out}. The median trend of $\Delta S/S_{out}$ is shown by the green dashed line and the blue envelope lines contain 68% of the galaxies. Dashed horizontal lines at $\Delta S/S_{out} = \pm 0.32$ mark the limits that define sources having good photometry. The intersection between the 68% envelope line and the good photometry limit defines the depths for Herschel data based on the simulations (red dotted line).

Comparison of different recipes

We also compare source extraction results of FASTPHOT to other techniques.



PSF-fitting
(Chary, Magnelli, et al.)

Figure 8: Here we plot the same figure as Figure, but for the PSF-fitting technique used by Chary, Magnelli et al.. The two techniques yield a comparable good photometry limit (red vertical dotted line), but the scatter at the bright end appears smaller for FASTPHOT. The reason may be that when running "normal" PSF-fitting, if two sources are too close to each other, e.g., with distance less than 1.5 pixels, we kept only the brightest one in the list of priors. This may cause the fitted flux to be overestimated.

Denoting clean sources with the covariance matrix

As can be seen in both Figures 2 and 3, there are many sources for which the output (fitted) flux deviates significantly from the input (actual) flux (i.e. unclean sources). The identification of these sources is one of the most important tasks in source extraction on Herschel maps, particularly on SPIRE maps.

As mentioned before, one of the advantages of FASTPHOT is that it calculates the covariance matrix. The diagonal terms of the covariance matrix are employed as the flux uncertainties. Given the list of priors and a noise map, these uncertainties represent the best accuracy we can get for each source, i.e., the real flux uncertainty can never be smaller than these values. It is thus possible to use these quantities to measure the quality of fit, and hence to identify clean and unclean sources.

To explore whether the flux uncertainties $\sigma_{S_{out}}$ given by FASTPHOT provide meaningful measurement of the accuracy of estimated flux, we conducted the following two experiments. First, we show the histogram of the distribution of $(S_{out} - S_{in})/\sigma_{S_{out}}$ for all the sources extracted from the simulated 250um map (Figure 9). If our derived $\sigma_{S_{out}}$ represents the real 1σ uncertainty of the estimated flux, the distribution of $(S_{out} - S_{in})/\sigma_{S_{out}}$ should form a Gaussian with σ=1, which is exactly the case.

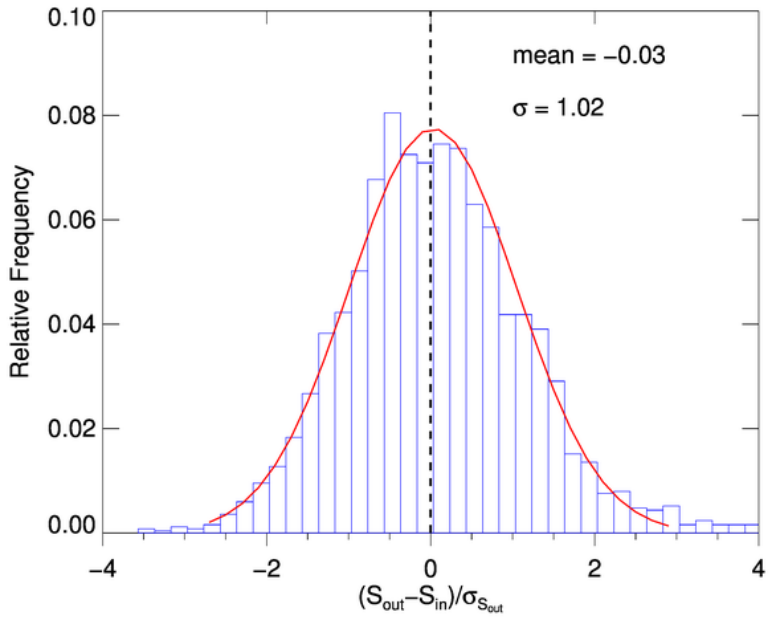


Figure 9: Histogram of $(S_{out} - S_{in})/\sigma_{S_{out}}$ *at SPIRE 250um.* $\sigma_{S_{out}}$ *is the flux uncertainty given by FASTPHOT,which is derived from the covariance matrix.*

Next we examine the consistency between $\sigma_{S_{out}}$ and the PAI ($\Delta S/S_{out}$) for individual sources, as shown in Figure 10. It is clear that sources with worse photometry accuracy tend to have larger $\sigma_{S_{out}}$.

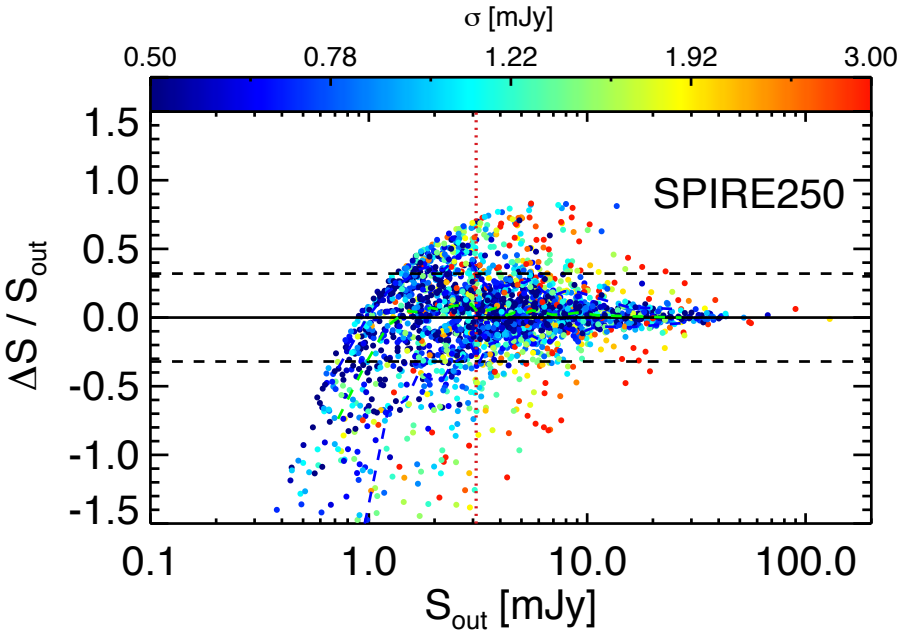


Figure 10: Same as Figure 7, but now sources are colour-coded by $\sigma_{S_{out}}$.

We define a critical σ_0, such that sources beyond the good photometry limit (the red dotted line in Figure 10) with $\sigma < \sigma_0$ would have a signal-to-noise ratio larger than 3. For 250μm maps, the good photometry limit is ~ 3mJy, thus $\sigma_0 = 1$mJy. To quantify the effectiveness of this method to correctly identify sources with good photometry ($|\Delta S/S_{out}| < 0.32$) in our simulations, we employed two parameters, the *purity* and the *completeness*. The *purity* measures the ratio of the number of good sources ($|\Delta S/S_{out}| < 0.32$) among sources selected by the criterion $\sigma < n * \sigma_0$ ($n = 1,2,3,5$), or *neib24* < 1,2,3,4, while the *completeness* (N_{good}/N_{total}) measures the ratio of the number of good sources amongst all the input sources at each flux bins. In Figure 11 and Figure 12 we plot the distribution of these quantities and compare them to other methods in previous works selecting good sources, which are mainly based on counting the number of bright neighbours.

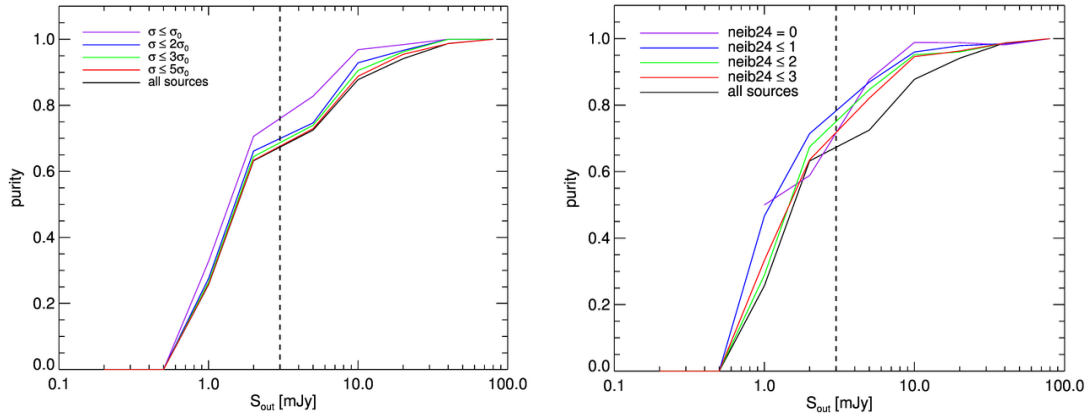


Figure 11: *Histograms of the purity for our method (left, based on measured flux uncertainty, σ) and that based on the number of 24um neighbors within 20" of the position of the prior, neib24 (right). The dotted line marks the good photometry limit. The distribution of purity for both methods is very similar, showing that either using the flux uncertainty or neib24 helps to improve the purity of the sample.*

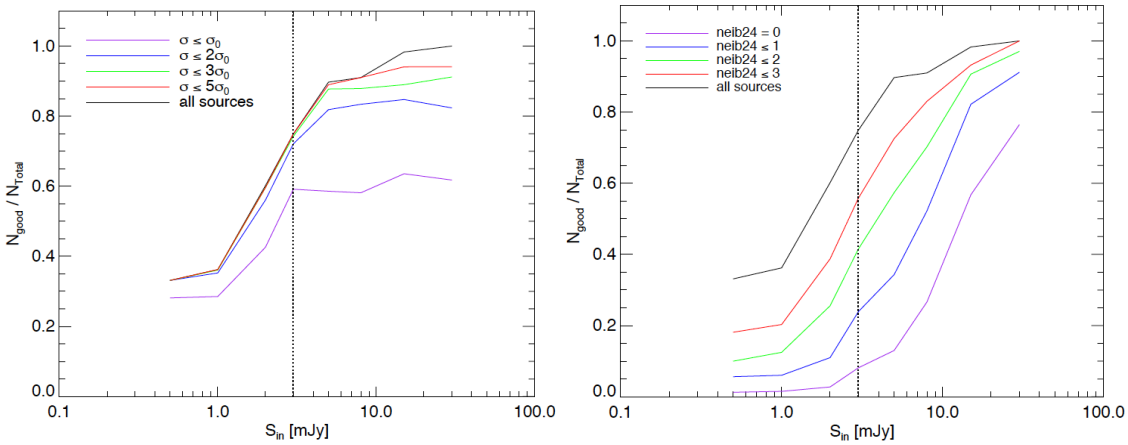


Figure 12: The distribution of the completeness *as a function of the input flux, S_{in}, for the two methods. While the use of flux uncertainty σ and* neib24 *to identify good sources reach similar purity, the former method yields a much higher completeness. For instance, at 3mJy, applying a cut of $\sigma \leq 2\sigma_0$ can select 70% of the good sources while applying a cut of $neib24 \leq 1$ only picks 25%. In the future, we will test this method in real images.*

9.3 Addendum to 3.2.3 The analysis of the 4Ms Chandra image of the CDF-S

Since the first trials we have applied several improvements to the software and to data analysis techniques discussed in the SW report. In particular we have improved the part of software that computes the source centroids since we noticed in the first release a shift in the positions of half a pixel. Moreover the software needs as input a background map, which was previously computed with a spline fit of the source-subtracted image. This method left spurious features in the background maps and therefore we decided to make use of the background templates provided by the Chandra X-ray data Center (CXC). Basically these are long exposures taken with the ACIS detector in stow mode so the only recorded events are instrumental events and particle background events. In practice is it a sort of dark image of the detector. The remaining part of the background (purely cosmic diffuse background), which unlike the particle background, suffers from the off-axis dependent vignetting has been modeled according to the exposure map. A full description of the method can be found in Cappelluti et al. (2013).
As we mention in the SW report, the literature contains a plethora of detection methods for X-ray surveys and no single one has been proved to be more efficient than the others. Within ASTRODEEP, in order to increase the number of X-ray detections with respect to what is already published, we have decided to combine three methods of source detection using, initially, the CANDELS GOODS-S field as a test field. The first method, which has been already published by Xue et al. (2012, X12), is the classic blind wavelet detection method provided by the CXC software *wavdetect*. We started by using the X12 output as a reference catalogue. Then in order to increase the number of detected X-ray sources, we performed a blind X-ray detection by pre-selecting a large number of background fluctuations isolated by a sliding cell technique with a signal-to-noise ratio (SNR) threshold SNR=2. The pre-selected sources have been fitted with *cmldetect* with the position, flux and extension as free parameters. Only sources exceeding the threshold DET ML=6 were included in the preliminary catalogue.
The third method makes use of the CANDELS GOOD-S W160 selected catalogue (Guo et al. 2013) as input for *cmldetect*. Several sources could be missed with an X-ray blind detection. By using this prior we increase the probability of detecting faint sources not previously detected by the pre-selection with the sliding-cell technique. Finally the catalogues have been combined with a simple position match. Unless otherwise stated, this stage of the analysis refers to the 0.5-2 keV energy band. Higher energy bands will be analyzed in the future when the procedure will be completely tested. We have therefore combined all the blind one/two stages detection and a two-stage detection using HST sources as a prior.

Blind X-ray detections
In order to compare our results to those of produced by X12, we ran a two-stage X-ray source detection by pre-selecting source candidates with the sliding cell software *eboxdetect* by fixing a signal-to-noise ratio (SNR) threshold SNR>2. The pre-selected sources were then PSF-fitted using *cmldetect* with flux, extension and position as free parameters. We included in the final catalogue all the X-ray sources with detection likelihood DET ML>6. As a result we detected 1157(1014) sources with more than 5(9) net-counts. If we cut the catalogue at DET ML>8 we find 709(656) source with 5(9) net-counts. The DET ML>6 catalogue has been matched with that produced by X12 with a search radius of 2". In the CANDELS area these methods detected 481 sources in the 0.5-2 keV band. 393(382) sources have common entries in both catalogues, with 88 present in the X12 catalogue only. When comparing the DET ML>8 catalogue with that produced by X12 we found, 375(368) common sources. 764(632) sources are detected with ≥5(9) counts with *cmldetect* only at a threshold DET ML≥6. 346(299) source are detected with ≥5(9) counts with *cmldetect* only at a threshold DET ML≥8. In order to assess the

capabilities and the improvements introduced by that technique we show in Figure 13 the comparison, for the 393 common sources, of the detected counts by *cmldetect* and by X12. It is clear that the agreement is excellent in every flux bin.
However previous studies suggest that, amongst all the available software, *cmldetect* provides the most reliable photometry (Puccetti et al. 2009). Also, Puccetti et al. (2009) have reported that, with Chandra data, wavelet algorithms are the most effective in terms of source positioning. Therefore in the final catalogue, if a source is detected both by X12 and *cmldetect* the position entry will be retained from X12 while the photometric information will be taken by *cmldetect*.

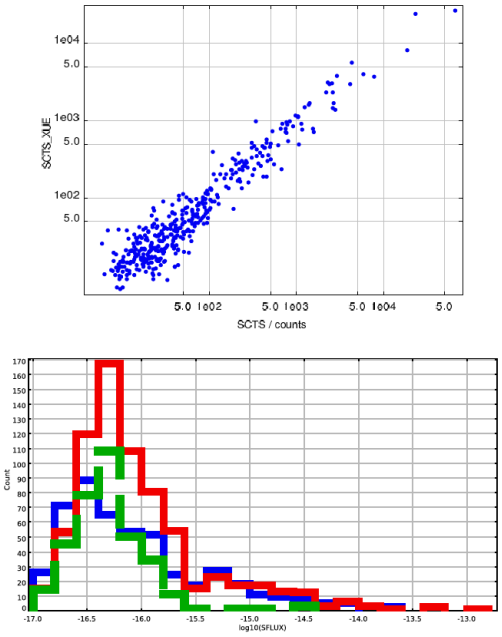


Figure 13. Comparison of the measured counts for the 393 sources detected both by cmldetect (on the x-axis) and by Xue et al 2012 (Y-axis). Bottom: The flux distribution of Xue et al. sources in blue and of all sources detected by cmldetect with DET_ML>8 and more than 5 counts. In green the distribution of the "new" sources detected by cmldetect ony.

We also checked the properties of the "new" sources by comparing the flux histograms of the X12, *cmldetect* and *cmldetect* only detection (with *cmldetect* threshold cut DET ML≥8 and more than 5 counts). As is clear from Figure 1, these are mostly faint sources peaking at log(S) ≈-16.4. In both catalogues the flux limit is of the order S_{lim} ≈10−17 erg s^{-1} cm^{-2}. In Figure 2 we show a cutout of the image showing "old (X12)" and new blind detection sources and it can be seen that new sources are easily detectable by eye.

Detection with HST-CANDELS GOODS-S sources as priors
As a third step we ran *cmldetect* using as an input catalogue the 34930 source positions from Guo et al. (2013) and fitting to the Chandra data. In principle using the positions of very deep H-selected sources would increase the probability of finding an X-ray source without relying on any statistical pre-selection method. Naively one could in principle perform source detection by fixing the position of the input source and fitting flux and extension, only. However this is not possible for two reasons, the first is that the binning of Chandra images and the PSF size are significantly larger that the angular resolution of HST. In addition, at the

TABLE 1. Number of detections for the two novel X-ray source detections with different threshold limits in *cmldetect*

Method	Threshold DET_ML	C_{min} cts	NTOT	NEW[a]
X12+*cmldetect*-Blind	6	5	1245	764
X12+*cmldetect*-Blind	6	9	1102	632
X12+*cmldetect*-Blind	8	5	827	346
X12+*cmldetect*-Blind	8	9	780	299
X12+*cmldetect*-Blind+HST Prior	6	5	1565	1084
X12+*cmldetect*-Blind+HST Prior	6	9	1267	885
X12+*cmldetect*-Blind+HST Prior	8	5	848	485
X12+*cmldetect*-Blind+HST Prior	8	9	773	416

[a] With respect to x12

magnitude limit of CANDELS, the source density of NIR-selected source is much higher that that of Chandra sources, and several HST sources can be found within (apparently) the same Chandra source. Since we are interested in finding new X-ray sources and then finding their best counterpart in the CANDELS catalogue, by fixing the positions in the source detection to those of the input catalogue we would bias the output toward faint and hence more numerous optical counterpart. To summarize, it is not possible to associate an X-ray flux using Chandra starting from an optical position if the optical telescope has an angular resolution much better than that of Chandra. A technique such as the likelihood ratio must be used to associate an X-ray source to its optical counterpart. However, in this part of the experiment we are solely interested in finding as many X-ray sources as possible, and the optical prior technique is potentially rewarding.

Other sources of contamination must be taken into account, for example, faint input sources could be confused with the wings of a bright off-axis source, or very close X-ray sources may not be resolved without correctly tuning the behavior of the software. For this reason we allowed the software to fit up to 10 input sources simultaneously within a radius corresponding to 90% of encircled energy. The software is capable of distinguishing whether multiple X-ray sources are associated with the input sources or if multiple optical sources appear associated with a single X-ray source. We set as a threshold DET ML=6 and removed all of the sources with less than 5 net counts. By correlating this catalogue with the X-ray blind detection catalogue we find 320(253) new soft X-ray sources with at least 5(9) net counts. At a threshold DET ML=8 we find 139(117) new sources down to a flux limit of ≈10−17 erg s^{-1} cm^{-2}. Therefore by combining the 3 methods we end up with a catalogue which included 476-1084 new X-ray sources depending on the chosen cut-off. However it is worth noticing that the improvement is not in the direction of pushing down the flux limit, but rather improving the efficiency of the survey. In any case, with the most conservative cuts in *cmldetect* we are able to at least double the number of X-ray sources in the GOODS- S field. In a forthcoming report we will report about the optical identification and the selection function of the new catalogue. All the results are summarized in Table 1.